npj | clean water

Article

Published in partnership with King Fahd University of Petroleum & Minerals

https://doi.org/10.1038/s41545-024-00352-3

Using static magnetic field to recover ammonia efficiently by DNRA process

Yuyang Xie[1], Zhibin Wang[1,2] & Shou-Qing Ni[1]

Dissimilatory nitrate reduction to ammonium (DNRA) has garnered attention due to its ability to recover ammonia and reduce greenhouse gas emissions simultaneously. In this study, the potential of using static magnetic field (SMF) to improve DNRA process was explored from the sight of molecular biology. Functional genes, microbial community structure, and metabolism pathways were discussed. SMF of 40 mT shortened the start-up time of DNRA from 75 days to 41 days, while 80 mT SMF delayed it to 103 days. On day 80, DNRA potential rate under 40 mT SMF, reached 174 ± 11 μmol kg^{-1} h^{-1}, significantly surpassing 0 mT (88 ± 6 μmol kg^{-1} h^{-1}) and 80 mT SMF (52 ± 4 μmol kg^{-1} h^{-1}). SMF of 40 mT also accelerated community succession and the enrichment of functional bacteria like *Geobacter* (from 15.71% to 32.11%). qPCR results suggested that 40 mT SMF promoted the rapid enrichment of DNRA functional gene *nrfA* and 80 mT SMF promoted the enrichment of *nirS* gene on day 40. Dynamic responses of *Thauera sp. RT1901, Stutzerimonas stutzeri*, *Shewanella oneidensis MR-1*, and *Shewanella loihica PV-4* to SMF at transcriptional levels confirmed SMF could improve the nitrogen removal and electron transfer of DNRA and denitrification bacteria. Consequently, this work validated the possibility of using SMF to improve DNRA process for ammonia recovery and investigated the underlying mechanisms, which could promote the application of DNRA in full-scale.

Ammonia (NH_3) plays a vital role as a key component in both food and fertilizer production, serving as a fundamental raw material for various industries and agricultural practices[1]. NH_3 also has garnered attention as a promising energy carrier in recent years[2]. Hence, the annual demand for ammonia has been on the rise. However, the current industrial process for synthesizing ammonia is known for its complexity, high energy requirements, and strong reliance on hydrocarbon feedstocks[3]. Currently, approximately 90% of commercially produced ammonia is obtained through the Haber-Bosch process, N_2 as its primary source, which is becoming increasingly restricted due to its non-flexible nature and risk of operation interruption[4]. In light of this, there is a critical and immediate demand for an ammonia generation process that is both clean and highly efficient, while consuming minimal energy. Nonetheless, the restricted solubility of N_2 in water and the high dissociation energy of the N ≡ N triple bond (941 kJ mol^{-1}) pose significant challenges, severely constraining innovative development and practical industrial applications[5]. On the contrary, the process of nitrate reduction to ammonia appears to hold greater promise as an approach for ammonia synthesis, considering its potential for enhanced NH_3 production efficiency and environmental protection[6]. Nitrate reduction to ammonia offers advantages in reaction thermodynamics and kinetics due to the lower N = O bond dissociation energy (204 kJ mol^{-1}) and faster nitrate (NO_3^-) mass transfer in water, which can facilitate large-scale ammonia production[7]. Converting widespread NO_3^- in groundwater or wastewater into NH_3 not only mitigates human health risks but also helps restore the global nitrogen cycle imbalance[8].

In wastewater treatment, biological processes have proven to be the most prevalent and successful methods for treating NO_3^-[9]. High nitrate-concentration wastewater has been perceived as a promising source for ammonia recovery[10]. In this respect, dissimilatory nitrate reduction to ammonium (DNRA), which could convert NO_3^- to NH_4^+ in two steps, may offer a possible solution[10]. Recent reports on the occurrence and contribution of DNRA in marine, inland water, soil systems, and wastewater treatment plants have greatly improved our understanding of the global nitrogen cycle[11,12]. Yuan et al.[13] found DNRA process predominated the nitrogen retention processes in the lake sediment at higher temperature and water depth[13]. Zhao et al.[10] utilized three carbon sources to successfully start up DNRA process and realize efficient nitrogen recovery[10]. Wan et al.[14] demonstrated the ammonia recovery efficiency of 44% via DNRA was achieved in microbial fuel cell[14]. Most wastewater treatment systems were originally designed for nitrate removal rather than recovery, leading to the dominance of conventional denitrification technologies[10]. Although

[1]School of Environmental Science and Engineering, Shandong University, Qingdao, Shandong, China. [2]School of Life Sciences, Shandong University, Shandong, Qingdao, Shandong, China. e-mail: sqni@sdu.edu.cn

denitrification process is the common pathway of N cycles, the importance of DNRA activity has been increasingly recognized due to the conservation efforts of available N form[13]. Furthermore, DNRA bacteria can reduce nitrite to ammonium, which is another substrate for anammox bacteria. Recent study reported that DNRA activities were used to reduce excess nitrite to ammonium to minimize nitrite toxicity to anammox bacteria[15]. However, the complicated carbon source competition and low growth rate of DNRA bacteria restrict the further investigation of DNRA to recover ammonia from wastewater[9]. Indeed, it is imperative to identify effective promotion strategies within bioreactors to drive DNRA outcompeting other processes.

Microorganisms possess intrinsic magnetism and can exhibit magnetic bioeffects induced by external magnetic fields, affecting enzyme activity and cell membrane permeability, and ultimately altering microbial metabolism[16,17]. The static magnetic field (SMF) has recently gained considerable attention due to its biological effects on wastewater treatment. SMF has been successfully applied in multiple biological wastewater treatment processes as an energy-free and no-secondary-pollution method. Filipic et al.[18] reported that SMF of 17 mT positively affected NH_4^+ oxidation and the growth of *Nitrosomonas europaea* in the laboratory pure culture[18]. Fan et al.[19] observed that SMF of 40 mT improved the nitrogen removal performance of anammox, especially under high nitrogen loading conditions[19]. Li et al.[20] developed a constructed wetland coupled with SMF for treating simulated wastewater and the results showed that 100 mT SMF significantly affected organics and nitrogen removal[20]. Considering the previous findings, it is reasonable to assume that SMF with suitable intensity could promote DNRA process.

This study investigated the possibility of utilizing SMF to enhance the DNRA process. The primary goal was to evaluate the long-term impact of SMF on DNRA. Quantitative real-time PCR (qPCR) technology was employed for estimating DNRA functional gene levels and Illumina MiSeq assays were utilized to investigate microbial community composition and function. In summary, this work aimed to present a cost-efficient, potent, and eco-friendly biotechnology for recovering ammonia from wastewater with elevated nitrate levels.

Results and discussion

Nitrogen conversion performance under different SMF

The ammonia nitrogen conversion efficiency of R1, which affected by 40 mT SMF, reached 50% within 41 days, indicating the successful start-up of DNRA process (Fig. 1b)[10]. Subsequently, R_{CK} successfully initiated DNRA over 75 days, while R2, which affected by 80 mT SMF, exhibited the longest initiation time of 103 days (Fig. 1a, c). Regarding initiation time, R1 was shortened by 45% compared to R_{CK}, whereas R2 was delayed by 27%. During the stable operational phase following successful initiation, the average ammonia conversion efficiency for R_{CK}, R1, and R2 were 58 ± 7%, 63 ± 6%, and 52 ± 8%, respectively (Fig. 1d). This indicated that after initiation, ammonia nitrogen conversion capabilities of R_{CK} and R1 were similar, with only a slight improvement by 40 mT SMF, but SMF intensity exerted inhibitory effects on DNRA. Regardless of SMF intensity, NO_3^- was almost consumed, whether through DNRA generating NH_4^+ or denitrification producing N_2, which could be due to the high COD/N ratio. Additionally, DNRA potential rates were determined on day 80, with R_{CK}, R1, and R2 being 88 ± 6, 174 ± 11 and 52 ± 4 μmol kg^{-1} h^{-1}, respectively (Fig. 1e). Although both R_{CK} and R1 successfully initiated DNRA process on day 80, higher DNRA potential rate was obtained in R1, which could be attributed to the higher abundance of DNRA bacteria in R1.

Effect of SMF on the bacterial diversity

Alpha-diversity indices were employed to disclose the microbial richness and diversity. As compared with R_{CK}, the fewer observed species, lower Chao1, and lower Shannon indexes observed in R1 and R2 indicated the lower richness and diversity of the community exposed to SMF (Fig. 2a). As the nitrogen conversion discussed above, the application of SMF selectively filtered the microbial communities: 40 mT SMF favored the proliferation of DNRA bacteria, whereas 80 mT SMF was more conducive to the growth of denitrifying bacteria. As a result, the diversity of communities subjected to SMF was lower than that of R_{CK}. A previous study demonstrated that the application of SMF to the A/O SBR process can decrease species diversity while promoting a more even and abundant distribution of species[21]. Hierarchical clustering analysis showed the similarity between the community composition of R1 on day 40 and R2&R_{CK} on day 80 (Fig. 2b), indicating that the SMF facilitated microbial community succession in R1.

Effect of SMF on the microbial community structure at phylum level

The main phylum was *Proteobacteria* (40.80–83.48%), followed by *Bacteroidetes* (4.29–13.41%) and *Chloroflexi* (3.11–8.19%) (Fig. 3a). *Proteobacteria, Chloroflexi*, and *Bacteroidetes* comprises bacteria that perform both denitrification and DNRA functions[22,23]. *Proteobacteria* was the predominant phylum in all samples, which was generally involved in the nitrogen cycle and contributed to COD removal in the wastewater treatment system[24]. On day 40, SMF of 40 mT significantly increased the relative abundance of *Proteobacteria* (66.83%) compared to the seed sample (45.50%), which exceeded R_{CK} and R2 by 64% and 39%, respectively. In the subsequent cultivation, the relative abundance of *Proteobacteria* in R1 was also higher than these in R_{CK} and R2. Considering the elevated DNRA activity of R1, it could be hypothesized that *Proteobacteria* was the primary phylum responsible for DNRA function within the reactor.

Effect of SMF on the microbial community structure at genus level

Geobacter, *Thauera*, and *SBR1031* were the main dominant genera in all samples except the seed sludge (Fig. 3b). *Geobacter* and *Thauera* belong to the phylum *Proteobacteria*. *Geobacter*, the dominant bacterium in three reactors, has been effectively enriched in the DNRA bioreactor, utilizing acetate as the carbon source[25]. During the cultivation process, the abundance of *Geobacter* in R1 consistently remained higher than in R2 and R_{CK}, and its growth rate was faster. On day 40, *Geobacter* had already become the dominant genus in R1 (15.71%), surpassing R_{CK} and R2 by 214% and 59%, respectively. On days 80 and 120, the relative abundance of *Geobacter* in R1 reached 22.57% and 32.11% respectively, significantly higher than R_{CK} and R2 during the same period. *Geobacter* appeared to be a key genus responsible for DNRA function within the reactor. As reported, *Geobacter* held a pivotal position in the environment due to its capability to incorporate organic and inorganic pollutants into oxidation and reduction pathways via metabolic reactions, respiratory chains, and sensory networks. It also regulated checkpoints to optimize growth efficiency to the fullest extent[26]. Previous study suggested *Geobacteraceae* was a crucial potential keystone member both in the DNRA and the entire bacterial community[27]. Specifically, *Geobacter spp*. were also notably recognized as electron transfer stations, facilitating the transport of electrons from organic matter to microbial acceptors[28]. *Thauera* was first enriched in R2 on day 40 (10.70%), followed by R_{CK} (6.23%) and R1 (4.69%). However, *Thauera* in R1 (18.93%) surpassed the levels in R_{CK} (14.44%) and R2 (16.44%) on day 120. *Thauera* has been reported as a type of DNRA bacteria, which contains all necessary genes encoding complete DNRA and canonical denitrification pathways[29]. *Thauera* was also an electroactive bacteria[30], which could perform extracellular electron transfer (EET). The genera *SBR1031* belongs to *Chloroflexi*, which has been documented for its capability to degrade aromatic compounds[31] and may play a vital role in the removal of extracellular peptides and cellular materials[32]. During the cultivation process, the relative abundance of *SBR1031* initially increased and then decreased. However, its relative abundance consistently followed the order: R1 < R2 < R_{CK}.

Moreover, it's worth noting that among the top 12 genera, the abundance of only three genera increased through cultivation, namely *Geobacter*, *Thauera*, and *Subgroup_7* (Fig. 3c). The abundance of seven genera increased initially and then decreased, which might result from the competitive interactions among different functional groups during community

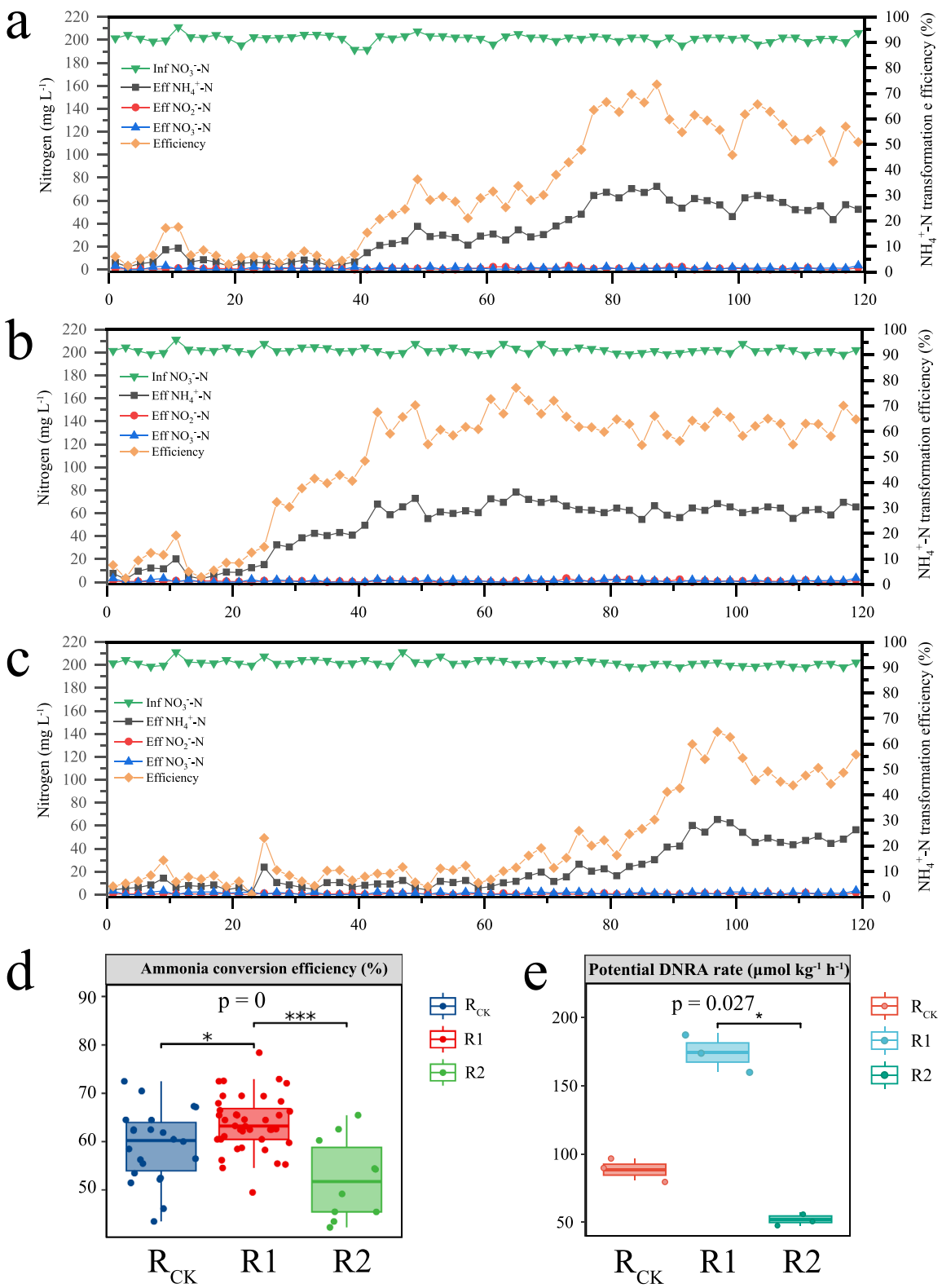

Fig. 1 | The nitrogen conversion performance under the effect of SMFs. The concentrations of nitrate, nitrite, and ammonium in (**a**) R_{CK}, **b** R1, and **c** R2 reactors in long-term operation were monitored. **d** Average ammonium conversion efficiency in three reactors. **e** Potential DNRA rates on day 80. Within the box, horizontal line denotes median value; box extend from the 25th to the 75th percentile of the group's distribution of values; vertical extending lines denote the most extreme values within 1.5 interquartile range of the 25th and 75th percentile of the group; dots denote observations. The significance of differences obtained by Kruskal–Wallis nonparametric test was indicated by asterisks: $p < 0.05$ (*), $p < 0.01$ (**), $p < 0.001$ (***).

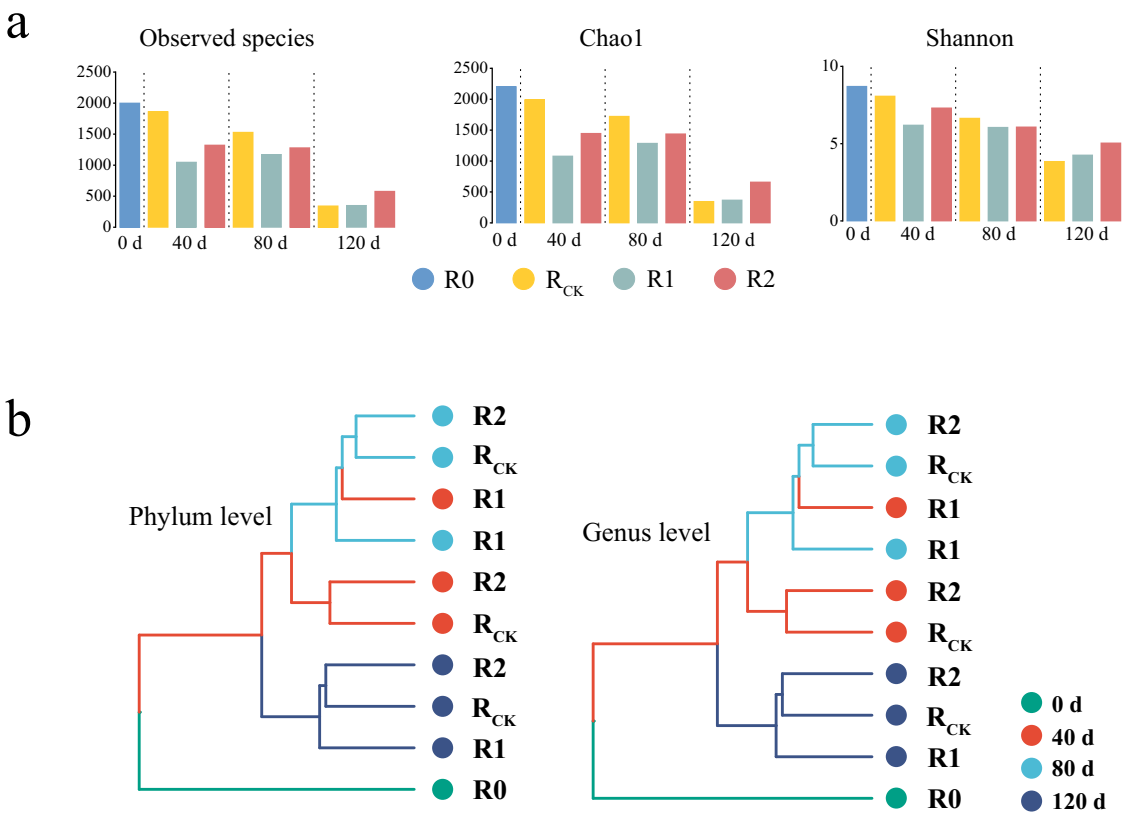

Fig. 2 | Effect of SMF on the bacterial diversity. a Bacterial diversity indexes and **b** hierarchical clustering analysis on the phylum and genus level.

succession. In the context of this study, the reactor environment was characterized as a low-nutrient environment. Consequently, over time, certain bacteria less adapted to the environment might gradually lose their nutritional competitiveness due to prolonged competition. Additionally, within these seven genera, most genera exhibited the lowest abundance in R1, indicating that the appropriate SMF enhanced the activity of certain bacteria, enabling them to gain dominance more rapidly and outcompete other bacteria.

Molecular ecological network analysis

Molecular ecological network analysis was conducted to investigate the co-occurrence patterns at three reactors (Fig. 3d). In R_{CK} and R1, all genera were divided into two modules. In contrast, they were divided into three modules in R2. *Geobacter* played a significant role in all three reactors. As previous study, *Geobacter* is proficient not only in oxidizing small molecular organic compounds like acetate, malate, and succinate but is also recognized for its capacity to facilitate interspecies electron transfer (IET)[33,34]. *Geobacter spp*. possess a substantial quantity of cytochrome c (cyt c) on the outer membrane, along with nanowires exhibiting metal-like conductivity, which have been reported to enhance EET[35]. Guo et al.[36] reported that the symbiotic interactions between *Geobacter* and denitrifying bacteria via IET contributed to the excellent performance of the biofilms[36]. Zhou et al.[37] reported SMF could promote the EET of *Geobacter*[37]. Similarly, in this work, the EET or IET capacity of *Geobacter* could be strengthened by SMF, driving *Geobater* to transfer electrons to other bacteria, which promoted overall microbial activity. Notably, *Geobacter* exhibited a consistent positive correlation with *Thauera*, although it showed predominantly negative correlations with most other genera in R_{CK} and R1. This suggested a potential symbiotic relationship between *Geobacter* and *Thauera*, with competition existing between *Geobacter* and other DNRA bacteria. In R_{CK}, R1, and R2, the proportions of the module containing *Geobacter* were 50%, 58%, and 25%, respectively. This trend aligned with the observed DNRA performance within the three reactors.

Effect of SMF on functional genes encoding key enzymes related to nitrogen cycle

To uncover the nitrogen metabolism in different stages, PICRUSt2 prediction was employed to identify functional genes associated with nitrogen transformation, utilizing the KEGG and COG databases (Fig. 4). Across all samples, a total of 22 functional genes associated with four nitrogen transformation processes were identified, including DNRA, denitrification, and anammox, respectively. *NrfAH* and *nirBD*, encoding nitrite reductase, key enzyme of DNRA process, presented the increasing trend in R1. On days 40 and 80, the relative abundances of *nrfAH* and *nirBD* in R1 exceeded those in R_{CK} and R2. Genes associated with denitrification (*nirK*, *nirS*, *nosZ*, *norBC*, *narGHI, napAB*) in R1 were all lower than R_{CK} and R2. By 120 days, the relative abundance of *nrfAH* in R1 remained higher than R_{CK} and R2, while a downregulation was observed in *nirBD*. *NrfAH* and *nirBD* enzymes are two main components of the nitrite regulation system of the cell, and it is known that *nirBD* is more active at high low nitrite levels, while *nrfAH* is more so at low nitrite levels[38]. In this work, nitrite was kept at low concentration (below detection line), thus *nrfAH* enzymes could be more active. Furthermore, on day 120, compared to R_{CK}, all denitrification genes in R1, except for *nirK*, were upregulated. Interestingly, the genes associated with anammox (*hzsABC*) were upregulated during the cultivation process. To be more specific, relative to the seed sludge, the *hzs* gene abundances in R_{CK}, R1, and R2 were upregulated by 180%, 313%, and 204% respectively. These genes exhibited a gradual and slight increase in expression throughout the subsequent cultivation. Reports have suggested that DNRA and anammox can coexist and even be coupled for nitrogen removal[39]. While anammox is fundamentally an inorganic autotrophic process, anammox bacteria can tolerate and utilize certain concentrations of organic carbon, even enhancing anammox activity[40]. Anammox bacteria also can use NO_3^- as an

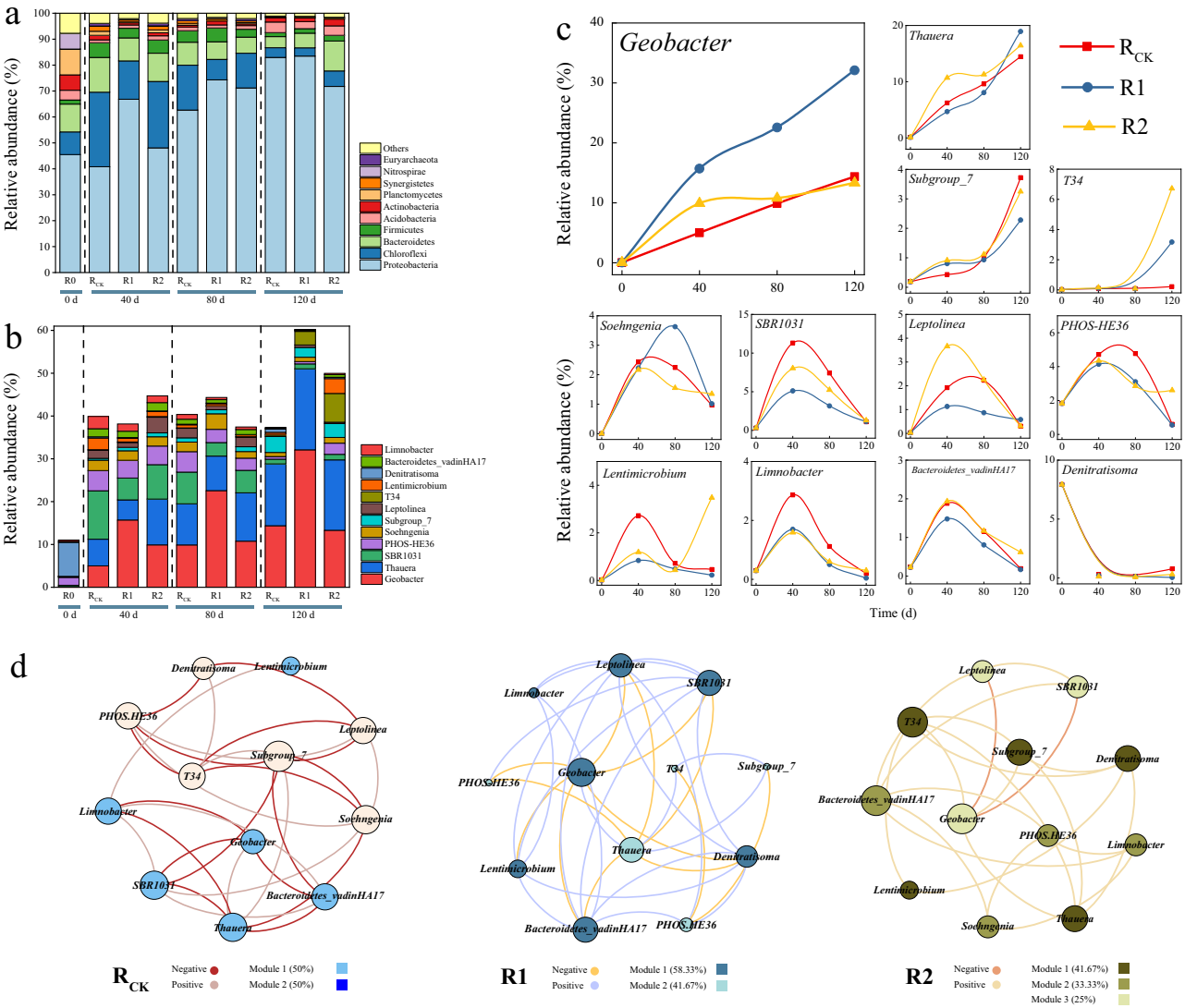

Fig. 3 | Effect of SMF on the microbial community structure. Microbial community structure on the (**a**) phylum and (**b**) genus levels. **c** The variation of the top 12 genera. **d** Ecological networks of the microbial communities under different SMFs. The colors of the nodes differentiate the different modules. The sizes of the nodes reflect the node degrees. The different lines indicate the positive and negative connections, respectively.

electron acceptor[41]. In this experiment, the low-carbon environment within the reactor may not inhibit anammox activity. Moreover, with both NH_4^+ and NO_3^- available as electron donors and acceptors, anammox bacteria were enriched initially in the R1 which contained more ammonium. Subsequently, the abundance of anammox bacteria also increased in R_{CK} and R2.

Network analysis and q-PCR results for functional genes

Network analysis was utilized to further investigate the relationship between microbes and nitrogen cycle functional genes (Fig. 5a). It is evident that *Geobacter*, *Thauera*, and *Bacteroidetes_vadinHA17* played critical roles in the reactor. Firstly, the close connection between *Thauera* and denitrification genes (*nirS*, *norBC*, *narGHI*) suggested that *Thauera* predominantly engaged in denitrification, aligning with previous reports[42]. Furthermore, *Geobacter* strongly correlated with *nrfA*, *nrfH*, and *nirB* genes, confirming its significant role in the primary DNRA function across the entire system. *SBR1031* and *Bacteroidetes_vadinHA17* strongly correlated with *nirBD* genes but not with *nrfAH* genes. Module_1 which contained *Bacteroidetes_vadinHA17* and *SBR1031* accounted for 44% and showed intricate connections, but module_3 which included *Geobacter* only accounted for 16%.

To further investigate the changes of DNRA and denitrifying bacteria throughout the cultivation stages under SMF, qPCR was conducted for validation. *NrfA*, the genetic marker for DNRA bacteria, was effectively enriched (Fig. 5b). On day 40, the abundance of the *nrfA* gene in R1 exceeded that in R_{CK} and R2, reaching 3.68×10^6 copies/ng DNA. It was 47% and 95% higher than these in R_{CK} and R2. Moreover, the abundance of *nrfA* continued to increase throughout the enrichment process, maintaining a dominant position in R1 among the three reactors. Studies indicated that the abundance of *nrfA* is directly proportional to DNRA activity[43]. In this study, R1, possessing the highest *nrfA* gene abundance, also exhibited the highest potential DNRA rate. As genetic markers for denitrifying bacteria, *nirK* and *nirS* exhibited distinct abundances in this study, with *nirK* being three orders of magnitude lower than *nirS*, which suggested that most denitrifying bacteria within the reactor were likely of the *nirS*-type (Fig. 5b). On day 40, denitrification genes in R2 had the highest abundance among the three reactors, exceeding the gene abundance in R_{CK} and R1 by 101% and 372%, respectively. However, on day 80, the abundance abruptly decreased to 4.85×10^7 copies/ng DNA. In R1, the abundance of the *nirS* gene continued to rise throughout the cultivation process, reaching 8.98×10^7 copies/ng DNA on day 120. Redundancy analysis (RDA) revealed that only *Geobacter* showed a significant correlation with the *nrfA* gene on day 40

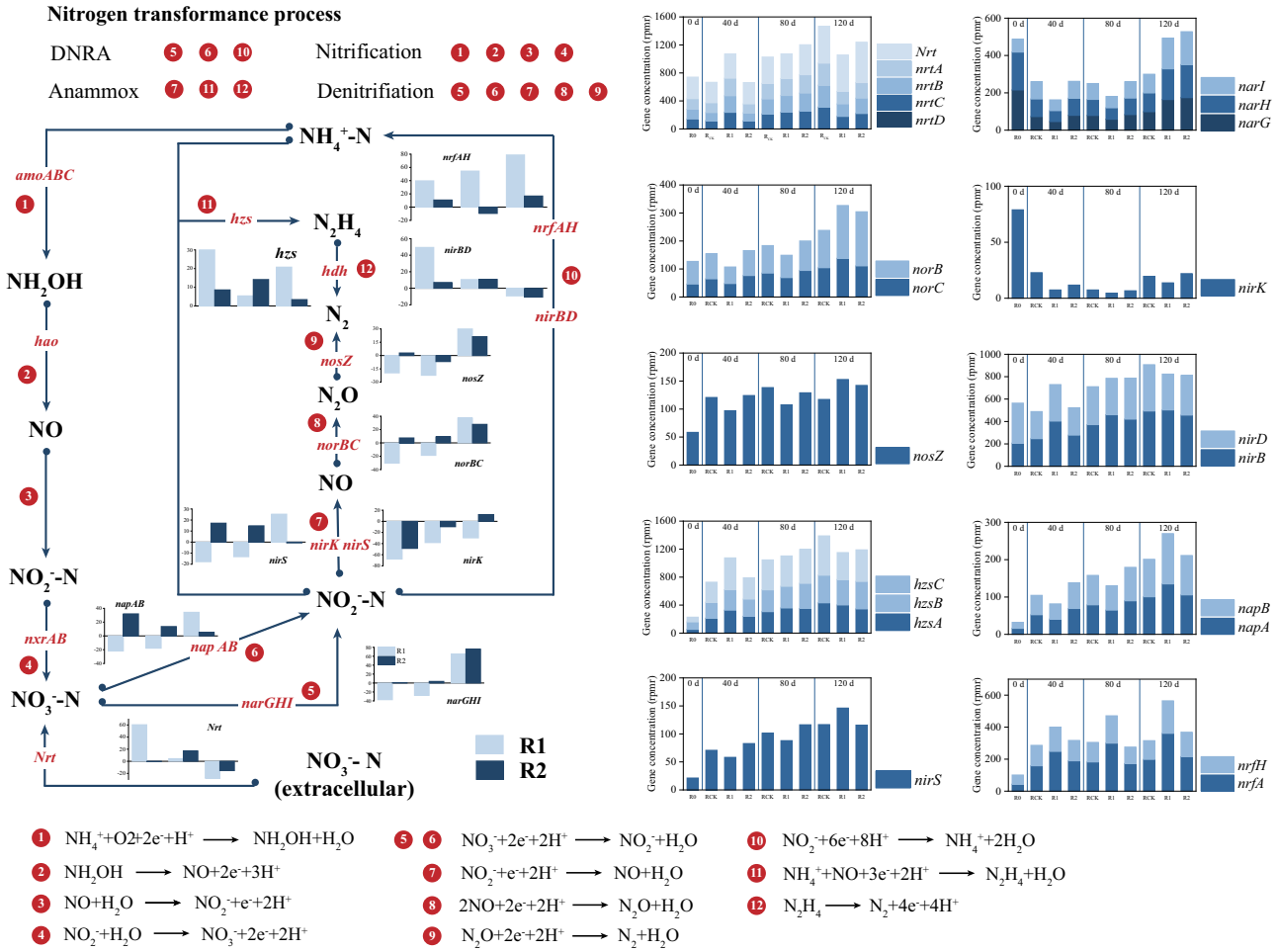

Fig. 4 | Relative abundances of genes encoding key enzymes for anammox, denitrification, and dissimilatory/assimilatory nitrate reduction. The abundance of genes in each sample is shown in colored bar charts. The data of *hzs*A, B, C were referenced from the COG database, while other gene data were referenced from the KEGG database.

(Supplementary Fig. 1). Most genera were positively associated with *nirS* and *nirK* genes. However, as time progressed, an increasing number of genera correlated with the *nrfA* gene, indicating a shift towards DNRA becoming the predominant function within the system. On days 40 and 80, *Thauera* exhibited a negative correlation with the *nrfA* gene, potentially due to its primary involvement in denitrification. It's worth noting that both denitrification and DNRA-related genes are inducible genes, meaning that they can not respond immediately to environmental changes[44]. Instead, they require a certain period of cycling to induce their expression. Moreover, many bacteria possess genes related to both denitrification and DNRA, such as *Shewanella loihica PV-4*[45]. Different environmental conditions induce these bacteria to execute various functions. Under conditions of high carbon ratios, DNRA demands a greater electron influx than the denitrification process. DNRA has an advantage over denitrification in nutrient-limited conditions, thus being more likely to dominate. The consistently strong correlation between R1 and the *nrfA* gene implied that the 40 mT SMF effectively promoted DNRA process. On the other hand, the negative correlation between *nrfA* gene and R2 during the initial 80 days, coupled with the positive correlation between R2 and *nirK/nirS* genes, suggested that the high SMF might influence bacterial gene expression, favoring denitrification and giving it a competitive edge over DNRA. This, in turn, could delay the initiation of the DNRA process.

Effect of SMF on microbial function

The trend of changes in microbial function was highly valuable for exploring the impact of SMF on the DNRA process. Throughout the operation, significant enrichment of bacterial chemotaxis, flagellar assembly, and two-component system was observed, predominantly under the influence of the 40 mT SMF (Fig. 6a). However, functions such as biosynthesis of ansamycins, biosynthesis of vancomycin group antibiotics, and protein export were downregulated. The co-occurrence network depicted intricate connections among the functions within the reactors (Fig. 6b). The selected functions were categorized into three modules. Examining the functions within each module, module_1 and module_3 predominantly encompassed nitrogen-sulfur-carbon metabolism and small molecule metabolism. Meanwhile, Module_2 primarily revolved around microbial energy acquisition, including flagellar assembly and bacterial chemotaxis. Module_2 mainly encompassed functions that were upregulated, including two-component system, bacterial chemotaxis, flagellar assembly, bacterial secretion system, riboflavin metabolism, and phosphotransferase system.

To further investigate the mechanisms underlying the promotion of the DNRA process under 40 mT SMF, a more in-depth analysis was conducted on the primary functions such as two-component system, membrane transport, cell motility, and EET on day 80 (Fig. 6c). Two-component system, widespread in microorganisms, perceives and transduces environmental information to trigger appropriate cellular responses, notably cell division, metabolism, cell motility, and electron transfer[46]. Compared to R_{CK}, R1 exhibited an upregulation of 18.83% in the two-component system. It also has been reported that the function activity of two-component system was enhanced under the SMF[47]. In this study, the 40 mT SMF enhanced the activity of the two-component system, which could be one of the reasons for the accelerated startup of

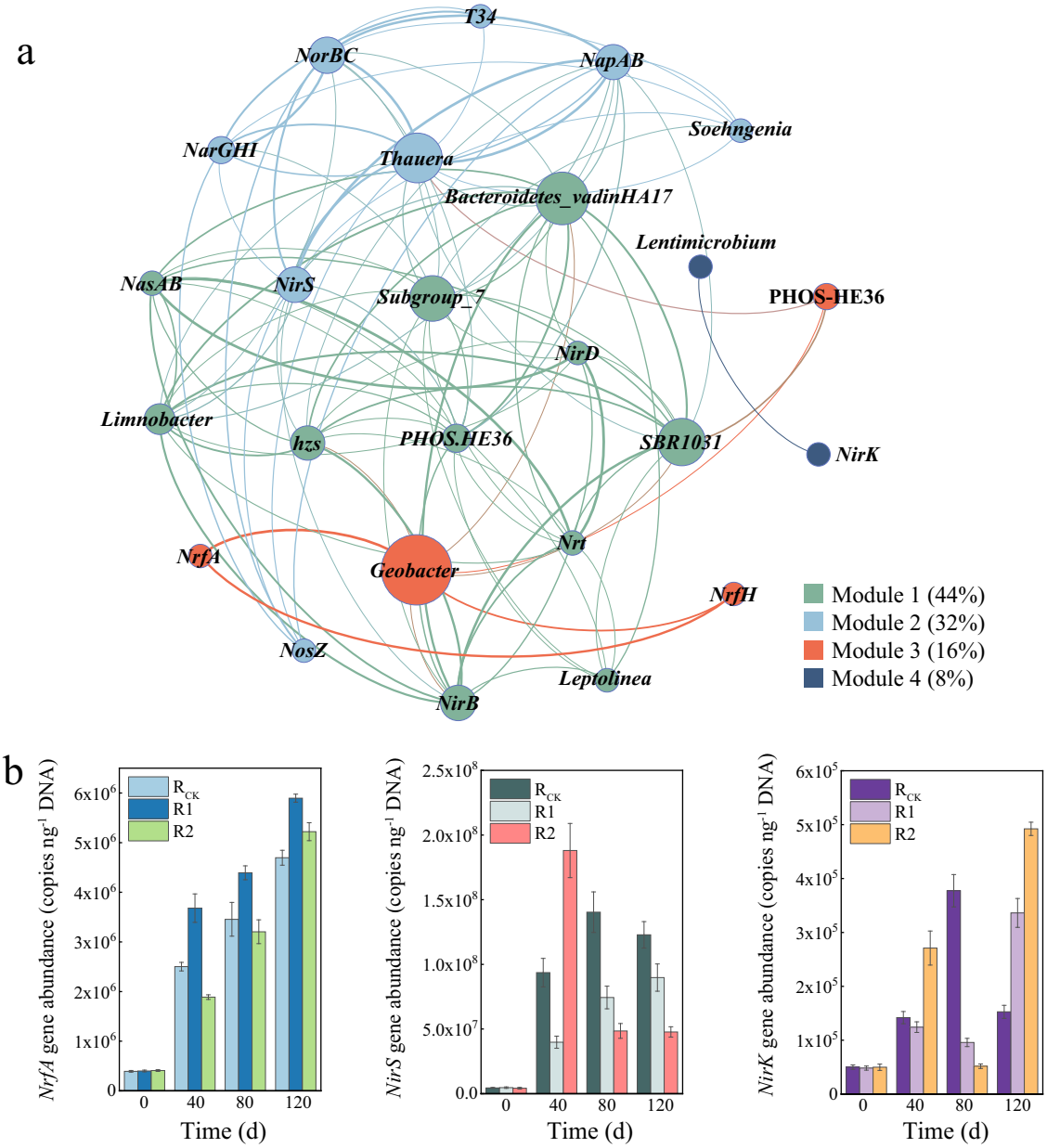

Fig. 5 | Relationships between dominant genera and nitrogen cycle genes. **a** Network analysis based on the relationship between dominant genera and functional genes. **b** q-PCR results for functional genes of *nrfA*, *nirS* and *nirK*. Data indicate average, and error bars represent standard deviation of the results from three independent sampling, each tested in triplicate.

DNRA. Moreover, compared to R_{CK}, R1 demonstrated an upregulation of 18.60% in the phosphotransferase system and 7.62% in the bacterial secretion system, both associated with membrane transport[47]. Cell mobility is a critical attribute for bacteria, enabling them to locate suitable niches even within challenging environments[48]. Under 40 mT SMF, flagellar assembly and bacterial chemotaxis, both related to cell motility, were upregulated by 27.27% and 43.41% compared to R_{CK}. Bacterial chemotaxis, in conjunction with flagellar assembly, empowers bacteria to navigate towards attractive substances or away from harmful chemicals. Consequently, these mechanisms are pivotal in orchestrating dynamic bacterial responses to diverse environmental conditions[49]. Sun et al.[50] reported that bacteria recruited to the rhizosphere via chemotaxis promoted NO_3^- acquisition in maize[50]. In this work, SMF was a likely regulator of bacterial chemotaxis. Under SMF, the rate of electron transduction through the flagella might be accelerated, increasing cell motility and prompting bacteria to capture nitrate ions more effectively, thereby enhancing DNRA efficiency. Notably, in this experiment, the dominant bacterial genera within the reactor, *Geobacter* and *Thauera*, were both electroactive bacteria[51], indicating the possible occurrence of EET. Studies have shown that riboflavin can stimulate anaerobic metabolism[52], bacterial biofilm formation[53], and EET[54]. There were reports indicating that the introduction of riboflavin into *Geobacter*-based co-cultures promoted IET by serving as an electron shuttle[55]. In this work, riboflavin metabolism was enhanced by 10.67% by 40 mT SMF, compared to no SMF irradiation.

Besides, certain functions in R2 were also upregulated compared to R_{CK}, including flagellar assembly, bacterial chemotaxis, and two-component system (Fig. 6c). In this experiment, compared to the control group, both high and low SMF demonstrated promotion of certain functions. This enhancement likely bolstered the microbial capacity to acquire nutrients and enhanced signal transmission, contributing to the enhancement of DNRA in R1 and denitrification in R2.

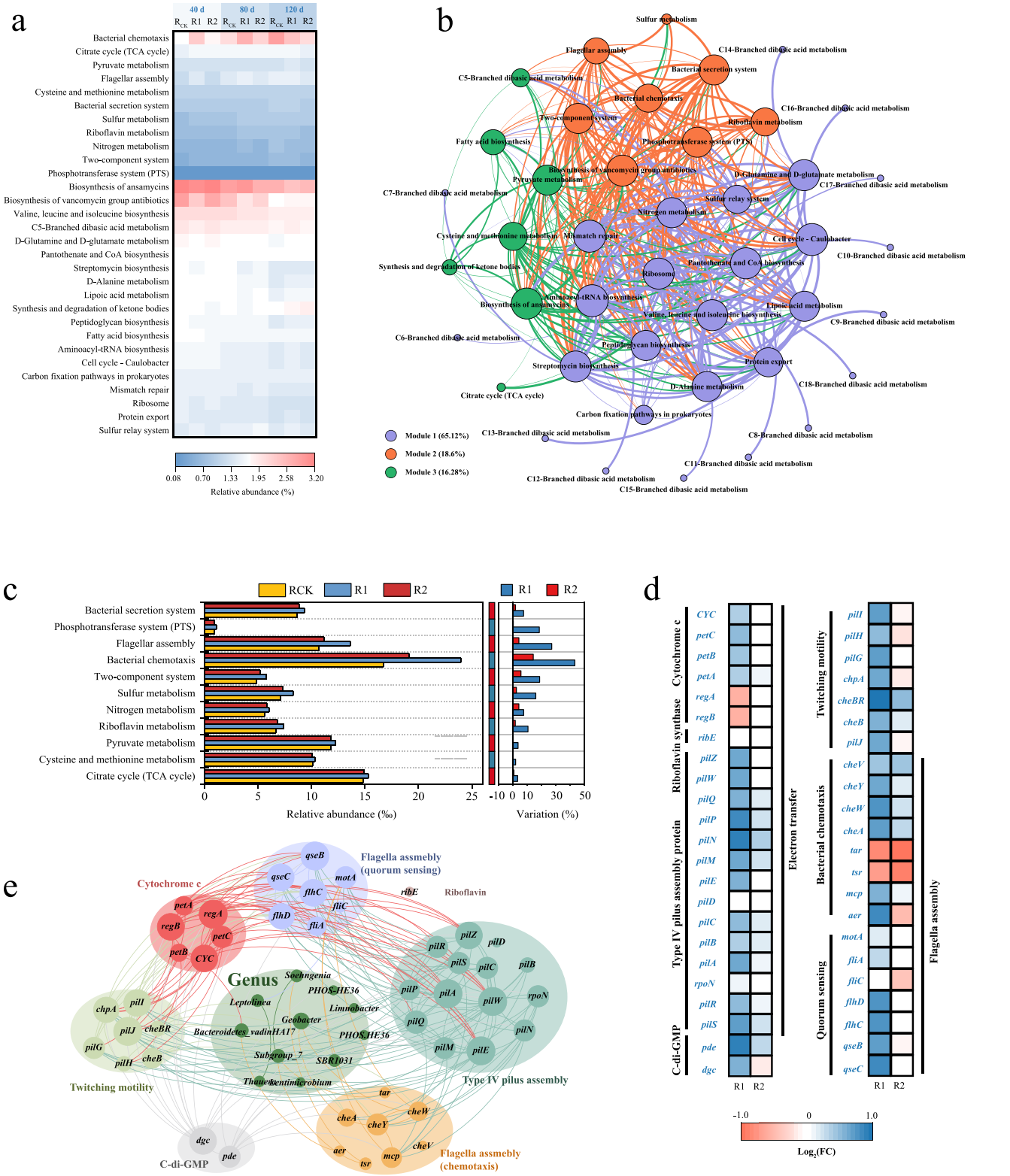

Fig. 6 | Analysis on the microbial function under SMF. a Heatmap and **b** co-occurrence network of KEGG pathways on the level_3. **c** Variation of selected KEGG pathways on day 80. **d** Heatmap of functional genes related to electron transfer and cell motility. **e** Molecular ecological network among functional genes and dominant genera on day 80.

Possible mechanisms

As discussed above, SMF primarily enhanced the microbial functions related to membrane transport, signal transduction, cell motility, and electron transfer. Concerning these functions, a search for the associated genes was conducted, aiming to uncover the connections among them (Fig. 6d, e). The two-component system is the most prevalent signal transduction mechanism, renowned for its ability to detect various stimuli and orchestrate rapid and appropriate responses, which encompass a wide array of functions such as bacterial communication, the synthesis of pili and flagella, as well as tolerance or reactions to external stress[56]. The two-

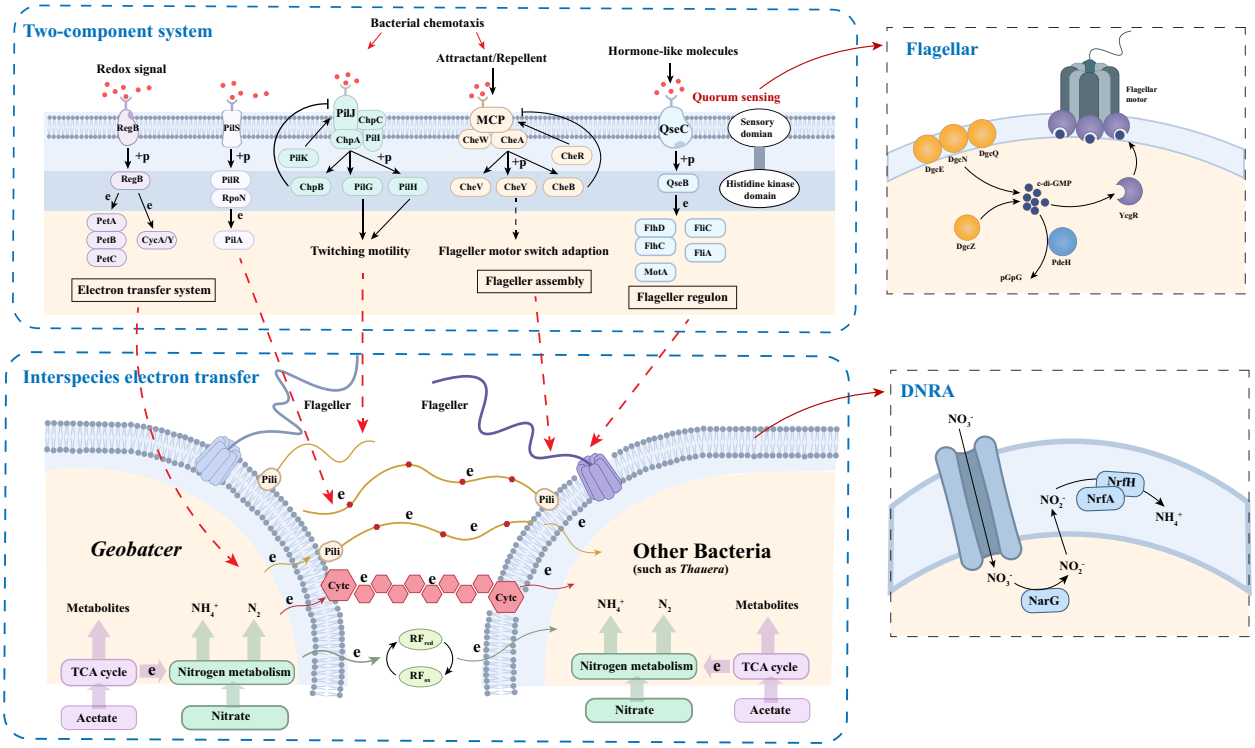

Fig. 7 | Possible mechanisms of SMF promotion on DNRA process. Under 40 mT SMF, two-component system regulated various functions, such as cell motility and extracellular electron transfer, via histidine kinase domain and sensory domain. Quorum sensing was influenced by SMF, regulating the flagellar motor. SMF possibly enhanced the interspecies electron transfer of *Geobacter*, enabling the transfer of electrons to other bacteria and further improving DNRA process.

component system consists of two essential proteins: a sensor protein housing the histidine kinase domain and a corresponding regulatory protein that contains the response regulator domain, as shown in Fig. 7[57]. Perception occurs in the periplasm or the extracellular space, within the membrane, or in the cytoplasm[58]. Genes related to electron transfer and cell motility within the two-component systems associated with signal transduction have been identified (Fig. 6d). However, due to the limitations of sequencing methods, no significant changes were detected in membrane transport-related genes. Most genes were upregulated under SMF influence, with a more pronounced effect in R1. The relevant genes in R2 appeared to be relatively stable, which indicated two-component system could be more likely activated under 40 mT SMF. The network analysis illustrated a close connection among genes of different functions (Fig. 6e). The dominant DNRA genus *Geobacter* was closely associated with type IV pilus assembly, twitching motility, and flagella assembly (chemotaxis).

Thus, as discussed above, two possible mechanisms based on two-component system were proposed: First, SMF accelerated extracellular electron transfer to enhance bacteria activity and bacterial motility; second, SMF improved bacteria motility to capture more COD and NO_3^-. R1 had an upregulation of genes related to type IV pilus assembly and cytochrome c (Fig. 6e). Hu et al.[21] found that applying SMF can improve TN removal efficiency of the A/O SBR process as the electron transport was enhanced[21]. Type IV pilus and cytochrome c are both essential components of EET systems. Considering that *Geobacter* possesses the ability of electroactivity[59], these findings suggested that 40 mT SMF likely enhanced the EET or IET capability of *Geobacter*, enabling the transfer of electrons to other bacteria. Network analysis revealed that the connections between *Geobacter* and other microbes in R1 were stronger compared to R_{CK} and R2. It consistently exhibited a positive correlation with *Thauera* in all three reactors (Fig. 3d). Based on the reported EET pathways[36], the first one is the e-pili mode, primarily through electron hopping and tunneling[60]. The second pathway is the cytochrome-to-cytochrome mode, in which electron transfer occurs only when the strains are in direct physical contact[61]. Hence, bacteria may accept electrons via some known cytochromes[62]. Third, electron shuttles like riboflavin might assist the electron transfer between the two consortia[63]. These pathways warrant further investigation into DNRA system.

The primary selective pressure driving the evolution of chemotaxis is the need to access nutrients[64]. Bacterial flagella and pili can sense adverse conditions, and chemotaxis can enhance bacteria's ability to access favorable environments[48]. Some species, like *Geobacter*, might exhibit comparatively slower substrate uptake and growth rates in comparison to other microbial populations. *Geobacter spp.* could be enriched under conditions of limited substrate competition, allowing them ample time to acquire the substrate with less competition from other microbial populations[65]. The ecological importance of cellular motility in enhancing NO_3^- use efficiency through DNRA pathway was reported in the plant rhizosphere[66]. In this experiment, the reactors were run in a low-carbon, and low-nitrogen environment, which compelled bacteria to enhance their activity for nutrient uptake. The SMF stimulation facilitated this process, driving bacteria to capture more substrate via cell motility. Additionally, the QseB/QseC system, recognized as an integral part of the regulatory apparatus of bacterial quorum sensing (QS), is indispensable for various bacterial life processes. It serves as the primary executor of swift responses that are crucial for bacterial survival in intricate and dynamic environments[67]. The intracellular quorum sensing signal molecules cyclic diguanylate (c-di-GMP) can help bacteria coordinate multiple metabolic activities such as bacterial movement. *Pde* and *dgc* genes, responsible for the decomposition and composition of c-di-GMP, were detected in this work. In this work, the relative abundance of pde was 75.65% higher than that of *dgc* (Fig. 6e), implying that c-di-GMP was broken down more rapidly than synthesized. As shown in Fig. 7, PdeH inactivated YcgR by keeping c-di-GMP levels low, thereby enabling flagella motor function[68].

The effect of SMF on nitrogen transformation of DNRA and denitrifying bacteria

Based on the discussion above, four bacteria which could perform denitrification or DNRA were selected to further investigate the effect of SMF.

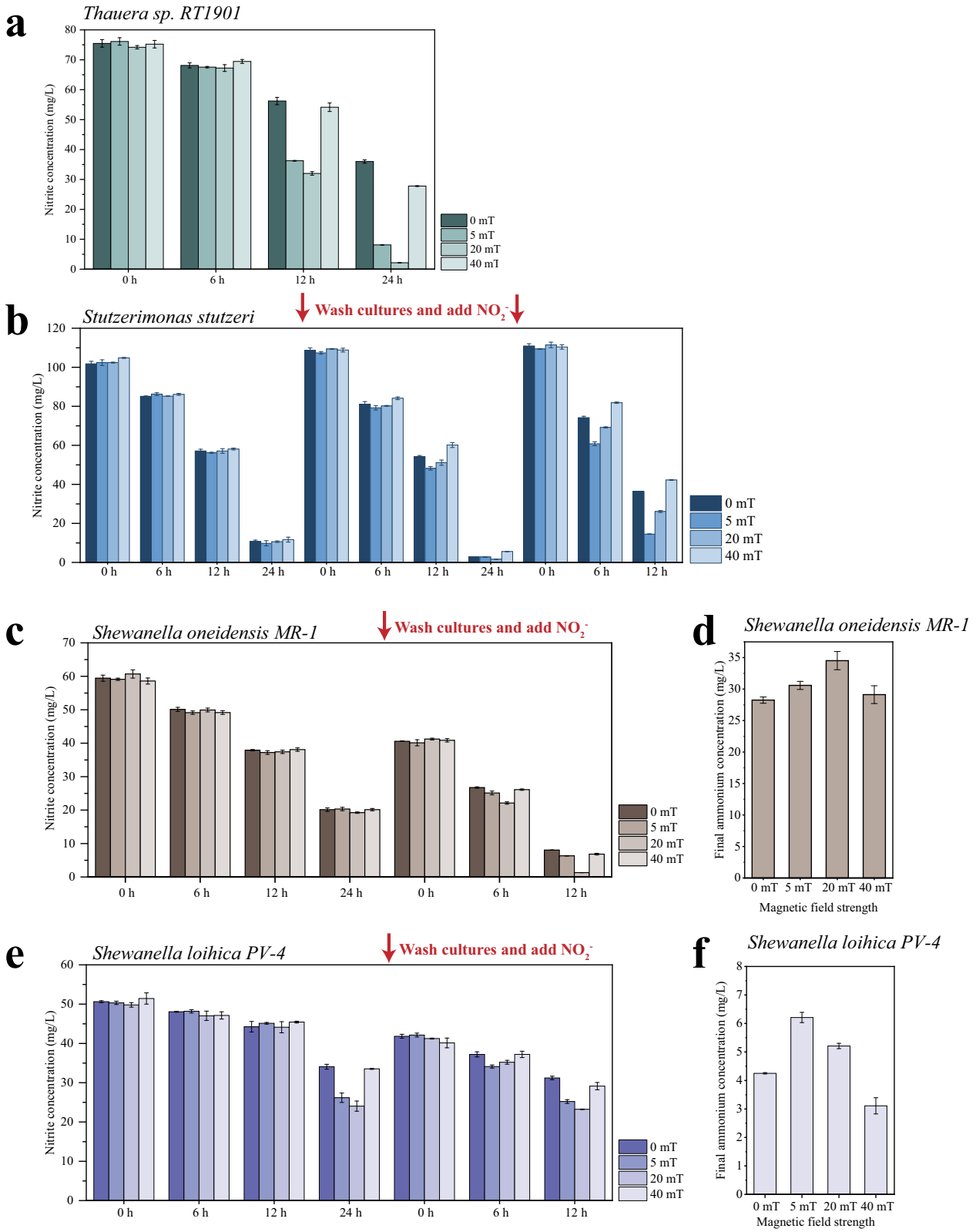

Fig. 8 | The nitrogen transformation performance of DNRA and denitrifying bacteria. The nitrogen transformation performance of (**a**) *Thauera sp. RT1901*, (**b**) *Stutzerimonas stutzeri*, (**c**, **d**) *Shewanella oneidensis MR-1*, and (**e**, **f**) *Shewanella loihica PV-4* under different SMF intensities were investigated. Data indicate average, and error bars represent standard deviation of the results from three independent sampling, each tested in triplicate.

Thauera sp. RT1901 and *Stutzerimonas stutzeri* could perform denitrification[69]. *Shewanella oneidensis MR-1* and *Shewanella loihica PV-4* were typical EET bacteria. *Shewanella oneidensis MR-1* could perform DNRA. *Shewanella loihica PV-4* possess the full genes for both DNRA and denitrification[69]. During the batch experiments, SMF affected the nitrogen transformation of DNRA bacteria and denitrifying bacteria (Fig. 8). Based on the results, *Thauera sp. RT1901* was the most susceptible to the effects of SMF due to the clear difference in nitrite removal at early 24 h, which might

be attributed to its diversified metabolism[69]. Moreover, SMF of 5 or 20 mT promoted the nitrogen transformation of all bacteria. SMF of 5 and 20 mT improved the nitrite removal of *Thauera sp. RT1901* by 72.3% and 82.5%, and *Stutzerimonas stutzeri* by 27.1% and 14.4%, respectively. SMF of 5 and 20 mT also enhanced the ammonia transformation of *Shewanella oneidensis MR-1* by 8.3% and 22.2%, and *Shewanella loihica PV-4* by 46.1% and 22.6%, respectively. However, 40 mT SMF had little enhancement for the nitrogen transformation, even inhibition for *Stutzerimonas stutzeri*. Thus, SMF could affect the nitrogen metabolism activity of bacteria, whether it is DNRA process or denitrification process, and the effects depended on the intensity of the SMF and the metabolic characteristics of the bacteria.

To further explore the dynamic responses of DNRA bacteria and denitrifying bacteria to different SMF, the transcriptional levels of functional genes related to nitrogen transformation and energy metabolism were analyzed (Fig. 9). *NirS*, *nirK*, *norB*, and *nosZ* were related to denitrification[70]. *NrfA* was the marked gene for DNRA[71]. *CcmFC*, *ccmFN*, and *ccmB* were related to electron transfer[72]. *Dgc-c* and *pde-c* were related to quorum sensing[73]. Based on the RT-qPCR results, an evident increase in the transcript level of DNRA and denitrification genes was observed under 5 and 20 mT SMF, consistent with the results of nitrogen transformation. *CcmFC*, *ccmFN*, and *ccmB* were also enhanced by 5 and 20 mT SMF, which suggested SMF could promote electron transfer and further enhanced nitrogen transformation. Previous researches have shown the positive role of the SMF in anaerobic digestion via promoting electron transfer process[74]. However, the expressions of *dgc-c* and *pde-c* were downregulated under 5 and 20 mT SMF. *Dgc* and *pde* were the major regulatory genes of c-di-GMP, which regulated cell movement, EPS secretion, and cell cycle progression. The lower expression of *dgc* and *pde* might lead to greater energy conservation in EPS secretion, bacterial proliferation, or other process. Consequently, nitrogen metabolism could access additional energy resources to advance further.

Application

In recent years, substantial global endeavors and investments have been aimed at advancing renewable energy sources. Industrial operations across different parts of the world have resulted in numerous direct and indirect adverse environmental outcomes. The widespread prevalence of nitrate wastewater holds a dual significance, potentially contributing to ecological harm while also presenting an opportunity for ammonia reclamation. In contrast to traditional nitrate removal methods, the implementation of DNRA provides the benefit of nitrogen recovery from nitrate wastewater while concurrently curbing the emission of the greenhouse gas N_2O from denitrification[10]. Ammonia can be easily separated from water based on its volatility and/or electrical mobility. Various methods had been reported to recover NH_4^+ from wastewaters including stripping[75], ion exchange, and forward osmosis[76]. Wu et al.[77] reported that the high pH (>12) at the catholyte further drove ammonium to ammonia gas, leading to a 96% ammonia recovery from synthetic reject water[77]. Kuntke et al.[78] used microbial fuel cell with a gas diffusion cathode to recover ammonia[78]. In the cathode chamber, ionic ammonium was converted to volatile ammonia due to the high pH. Ammonia was recovered from the liquid–gas boundary via volatilization and subsequent absorption into an acid solution. Thus, ammonia could be recovered as an energy carrier by ammonium. Moreover, DNRA has been considered a viable nitrite- and ammonia-generating mechanism from nitrate in an anammox bioprocess and has been used in various bioreactor setups to enhance anammox nitrogen removal[79]. Ammonium produced by the DNRA process could serve as substance for anammox process directly.

This work realized a high ammonium conversion efficiency in DNRA system improved by SMF. Compared with the other methods, the use of SMF induced by permanent magnets in the wastewater treatment process could provide several advantages such as no secondary pollution, no need for additional energy[80], cost savings[81], and ease of management and operation[82]. However, regarding its suitability for industrial and municipal wastewater treatment, the utilization of permanent magnets to establish a stable, constant magnetic field poses challenges and safety concerns. Ahmad et al. (2023) demonstrated an alternative approach by utilizing an iron core within the coil, powered by direct current, to generate the SMF[83]. This method opens avenues for employing magnetic beads and other magnetically-based carriers as support materials for biofilm formation, with the aim of enhancing bacterial activity through the generated magnetic field[84]. Despite the potential costliness of constructing such magnetic systems, the resultant magnetic field has shown significant benefits, including enhanced biological activity, improved bacterial resilience against substrate shock, and enhanced nitrogen removal performance[83]. Further investigation is warranted into optimizing reactor volume, type, and material, as well as magnetic field intensity, and the size and quantity of permanent magnets, to effectively manage the costs associated with the magnetic system.

The effects of SMF on DNRA process were systematically investigated in this study. 40 mT SMF could shorten the start-up time of DNRA process by the rapid enrichment of functional genes and the swift dominance of functional bacteria. *Geobacter*, as electroactive and DNRA bacteria, was most abundant under 40 mT SMF. Moreover, the underlying mechanisms were also discussed in this work: 40 mT SMF could improve DNRA process by stimulating a range of microbial functions, including energy metabolism, cell motility, electron transfer, and membrane transport. RT-qPCR results indicated that SMF could affect the nitrogen metabolism activity of bacteria and the effects depended on the intensity of the SMF and the metabolic characteristics of the bacteria. This study proved the feasibility of improved ammonia recovery efficiency via DNRA process by applying SMF and provided an economic method for the application of DNRA process in real-wastewater treatment plants.

Methods

Reactor set-up, synthetic medium, and inoculation

To enrich DNRA bacteria, three parallel sets of non-woven fabric membrane bioreactors (nMBRs) were designed (Supplementary Fig. 2). The SMF generation device was two rubidium magnets placed in parallel and one below the reactor. This device could produce 0-80 mT SMF inside the reactor, which has bio-affinity. In this experiment, R_{CK} was the control reactor, R1 was irradiated by 40 mT SMF, and R2 was irradiated by 80 mT SMF. SMF intensity distribution inside the reactor was shown in Supplementary Fig. 3. The composition of synthetic wastewater was determined as the previous study[25], with slight modification (Supplementary Table 1 and Supplementary Table 2). The carbon source was acetate and the ratio of COD/NO_3^- was 7.7. To maintain anaerobic environment, the synthetic wastewater buckets were purged with high-purity nitrogen gas for 20 minutes daily. The concentrations of nitrogen compounds (NH_4^+-N, NO_2^--N, and NO_3--N) were determined using the Standard Methods[10].

^{15}N tracer incubations, DNA extraction, and real-time qPCR analysis

The potential rate of the DNRA process was assessed by conducting slurry incubation experiments using ^{15}N isotope tracing technology, which allowed for precise measurement and tracking of nitrogen transformations as previous work[10]. The extraction of genomic DNA from the sludge samples was performed using the DNeasy Power Soil DNA Kit (Qiagen, Germany) following the manufacturer's instructions. The DNA quantification was carried out using an ultraviolet microspectrophotometer (K5500, Kaiao, China). DNA samples were stored at −20 °C for preservation and subsequent experiments. Quantitative real-time PCR (qPCR) was employed to assess the abundance of target genes in the three reactors. All functional genes were quantified by a qPCR system (Roche Light Cycler 480, Switzerland) using manufacturer software. The *nrfA* gene, responsible for encoding nitrite reductase enzymes, was used as a molecular marker to quantify DNRA bacteria. *nirS* and *nirK*, accountable for reducing NO_2^- to NO, were used as biomarkers for denitrifying bacteria[85]. The qPCR analysis was performed according to Zhao et al.[10]. Specific primers (Supplementary Table 3) and PCR programs (Supplementary Table 4) for target genes in qPCR was provided.

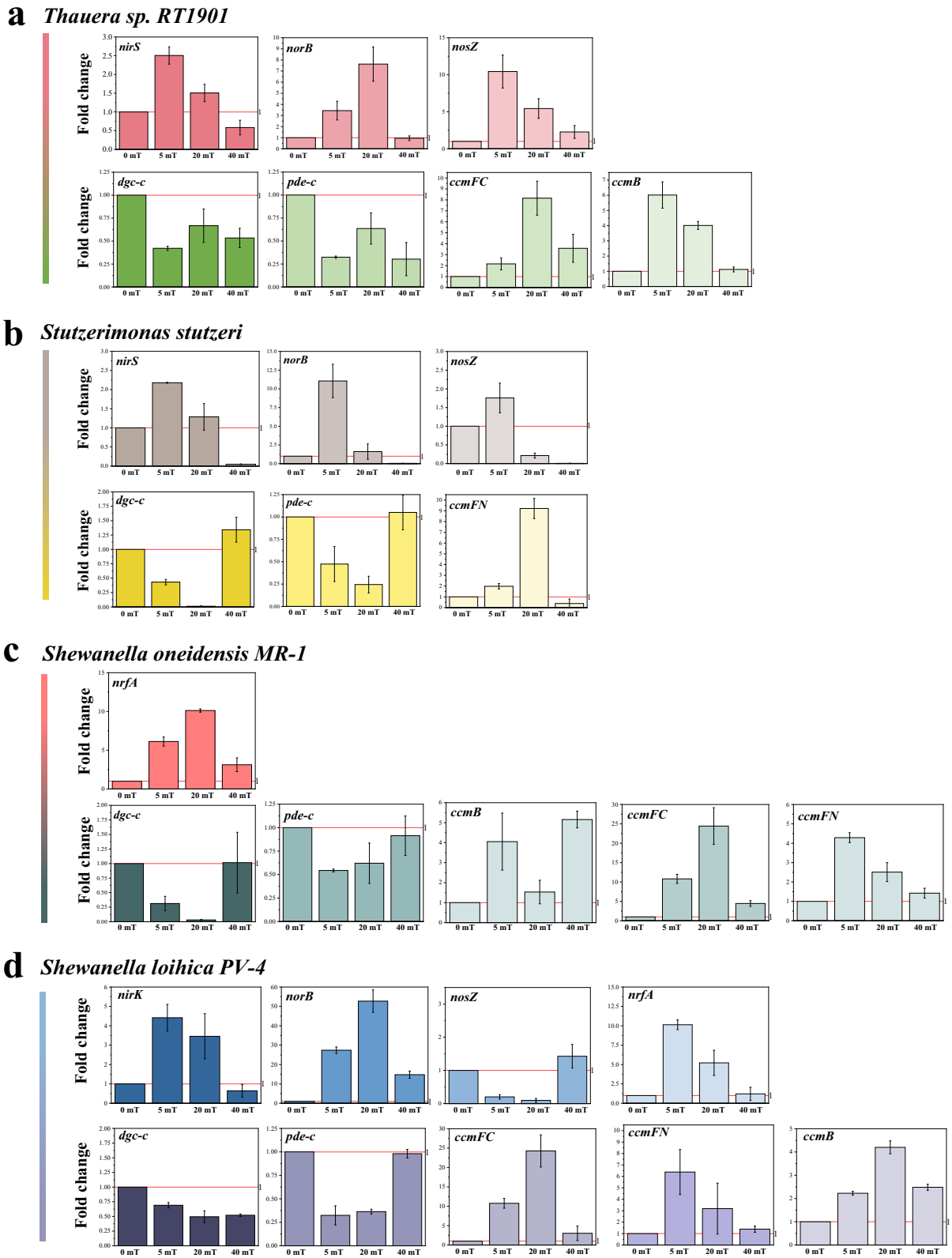

Fig. 9 | The RT-qPCR results of the functional genes. The genes related to nitrogen transformation and energy metabolism of **(a)** *Thauera sp. RT1901*, **(b)** *Stutzerimonas stutzeri*, **(c)** *Shewanella oneidensis MR-1*, and **(d)** *Shewanella loihica PV-4* under different SMF intensities were tested at transcription level. Fold change <1 means gene downregulation and Fold change >1 means gene upregulation. Data indicate average, and error bars represent standard deviation of the results from three independent sampling, each tested in triplicate.

Amplification PCR and high-throughput sequencing

The 16S-rRNA gene was amplified by PCR, using the barcode-primers set 515 F (5′-TWNGGCATRTGRCARTC-3′) / 907 R (5′-CCGTCAATTCMT TTRAGTTT-3′)[86]. The 2% agarose gel electrophoresis method was used to detect the PCR amplification products using the gel purification kit (AXYGEN, USA) for fragment excision and recovery. Then, Microplate reader (FLx800, BioTek, USA) and Quant-iT PicoGreen dsDNA Assay Kit were used to fluorescently quantify the amplified recovery products. The PCR amplicons were subjected to 2 × 300 bp paired-end sequencing using the Illumina NovaSeq platform. PICRUSt2 was used to predict the potential of a sample using 16 S rDNA amplicon sequencing. KEGG Orthology (KO) was used to classify all homologous genes to a specific gene whose function is known to be in the same category[87].

The effect of SMF on functional bacteria

Thauera sp. RT1901, *Stutzerimonas stutzeri*, *Shewanella oneidensis MR-1*, and *Shewanella loihica PV-4* were selected for nitrogen transformation experiments. The nitrogen transformation accumulation medium contained the following components: 0.5 g L^{-1} sodium acetate, 0.2 ~ 0.5 g L^{-1} sodium nitrite, 1.0 g L^{-1} NaCl, 0.5 g L^{-1} $MgCl_2$, 0.3 g L^{-1} KCl, 0.015 g L^{-1} $CaCl_2$, and 1 mL L^{-1} trace element solution[69]. The Luria broth (LB) medium included 10.0 g L^{-1} peptone, 5.0 g L^{-1} yeast extract, and 10 g L^{-1} NaCl. Single colony of *Thauera sp. RT1901*, *Stutzerimonas stutzeri*, *Shewanella oneidensis MR-1*, and *Shewanella loihica PV-4* was inoculated into 300 mL the LB medium and cultured at 30 °C for 24 h with agitation to encourage growth. After activation, the cultures were centrifuged at 8000 rpm, washed three times with sterile phosphate-buffered saline (PBS) and ultrapure water, and resuspended in the nitrogen transformation medium. Then the cultures were dispensed in serum bottles with an effective volume of 100 mL, and control the concentration of the bacterial solution at OD_{600} = 0.2 – 0.3. By adjusting the distance between the serum vials and the permanent magnet, the SMF intensity at the center of the serum vial was set to 0 mT, 5 mT, 20 mT, and 40 mT. If the batch experiments do not get obvious experimental results at 24 h, PBS buffer will be utilized to wash the culture and nitrogen transformation medium will be added again. At the end of the batch experiments, the cultures were centrifuged at 8000 rpm and then RNA was extracted and reverse transcribed using the PerfectStart Uni RT&qPCR kit (TransGen Biotech Co., Ltd. China). Reverse transcription qPCR (RT-qPCR) was performed to quantify the gene expression level of functional genes by the Roche Light Cycler 480 Real-Time PCR system (Switzerland). The primer sequences of functional genes used in the RT-qPCR were placed in Supplementary Table 5.

Data availability

The data that support the findings of this study are available from the corresponding author upon reasonable request. The 16 S rRNA gene sequences obtained in this study were submitted to the NCBI Sequence Read Archive (SRA) under accession numbers SAMN41404876–SAMN41404895.

Code availability

The codes generated and/or used during the current study are available from the corresponding author upon reasonable request.

Received: 4 January 2024; Accepted: 24 June 2024;
Published online: 02 July 2024

References

1. Wang, J. et al. Performance and mechanism of ammonia production by electrocatalytic nitrate reduction based on dodecahydro-closo-dodecaborate hybrid. *J. Colloid Interface Sci.* **652**, 945–951 (2023).
2. Hasan, M. H. et al. A comprehensive review on the recent development of ammonia as a renewable energy carrier. *Energies* **14**, 3732 (2021).
3. Pattabathula, V. & Richardson, J. Introduction to ammonia production. *Chem. Eng. Prog.* **112**, 69–75 (2016).
4. Bouaboula, H. et al. Addressing sustainable energy intermittence for green ammonia production. *Energy Rep.* **9**, 4507–4517 (2023).
5. Zhao, J. et al. Zn single atom on N-doped carbon: highly active and selective catalyst for electrochemical reduction of nitrate to ammonia. *Chem. Eng. J.* **452**, 139533 (2023).
6. Yu, C. Q. et al. Managing nitrogen to restore water quality in China. *Nature* **567**, 516–520 (2019).
7. Hirakawa, H., Hashimoto, M., Shiraishi, Y. & Hirai, T. Selective nitrate-to-ammonia transformation on surface defects of titanium dioxide photocatalysts. *ACS Catal.* **7**, 3713–3720 (2017).
8. Shih, Y. J., Wu, Z. L., Huang, Y. H. & Huang, C. P. Electrochemical nitrate reduction as affected by the crystal morphology and facet of copper nanoparticles supported on nickel foam electrodes (Cu/Ni). *Chem. Eng. J.* **383**, 123157 (2020).
9. Pandey, C. B. et al. DNRA: a short-circuit in biological N-cycling to conserve nitrogen in terrestrial ecosystems. *Sci. Total Environ.* **738**, 139710 (2020).
10. Zhao, Y., Li, Q., Cui, Q. & Ni, S.-Q. Nitrogen recovery through fermentative dissimilatory nitrate reduction to ammonium (DNRA): carbon source comparison and metabolic pathway. *Chem. Eng. J.* **441**, 135938 (2022).
11. Wang, S. et al. Hotspot of dissimilatory nitrate reduction to ammonium (DNRA) process in freshwater sediments of riparian zones. *Water Res.* **173**, 115539 (2020).
12. Zhao, Y. et al. Survey of dissimilatory nitrate reduction to ammonium microbial community at national wetland of Shanghai, China. *Chemosphere* **250**, 126195 (2020).
13. Yuan, H., Cai, Y., Wang, H., Liu, E. & Zeng, Q. Impact of seasonal change on dissimilatory nitrate reduction to ammonium (DNRA) triggering the retention of nitrogen in lake. *J. Environ. Manag.* **341**, 118050 (2023).
14. Wan, Y. et al. Bioelectrochemical ammoniation coupled with microbial electrolysis for nitrogen recovery from nitrate in wastewater. *Environ. Sci. Technol.* **54**, 3002–3011 (2020).
15. Qiao, X. et al. Specific denitrifying and dissimilatory nitrate reduction to ammonium bacteria assisted the recovery of anammox community from nitrite inhibition. *Front. Microbiol.* **12**, 1–13 (2022).
16. Jia, W. et al. Response of nitrite accumulation and microbial characteristics to low-intensity static magnetic field during partial nitrification. *Bioresour. Technol.* **259**, 214–220 (2018).
17. Weaver, J. C., Vaughan, T. E. & Martin, G. T. Biological effects due to weak electric and magnetic fields: the temperature variation threshold. *Biophys. J.* **76**, 3026–3030 (1999).
18. Filipic, J., Kraigher, B., Tepuš, B., Kokol, V. & Mandic-Mulec, I. Effect of low-density static magnetic field on the oxidation of ammonium by Nitrosomonas europaea and by activated sludge in municipal wastewater. *Food Technol. Biotechnol.* **53**, 201–206 (2015).
19. Fan, W. et al. Enhancing anammox nitrogen removal by static magnetic field exposure: performance, microbial community and symbiotic relationship analysis. *J. Water Process Eng.* **53**, 103709 (2023).
20. Li, M., Zhang, J., Liang, S., Li, M. & Wu, H. Novel magnetic coupling constructed wetland for nitrogen removal: enhancing performance and responses of plants and microbial communities. *Sci. Total Environ.* **819**, 152040 (2022).
21. Hu, B. et al. Effects of static magnetic field on the performances of anoxic/oxic sequencing batch reactor. *Bioresour. Technol.* **309**, 123299 (2020).
22. Wang, Y. & Li, Q. Competition and interaction between DNRA and denitrification in composting ecosystems: insights from metagenomic analysis. *Bioresour. Technol.* **381**, 129140 (2023).
23. Wang, Z. et al. Enrichment of DNRA bacteria: shift of microbial community and its combination with anammox to promote TN removal. *J. Environ. Chem. Eng.* **10**, 108867 (2022).
24. Zhang, H. et al. Geographical patterns of nirS gene abundance and nirS-type denitrifying bacterial community associated with activated

sludge from different wastewater treatment plants. *Microb. Ecol.* **77**, 304–316 (2019).
25. Van Den Berg, E. M., Van Dongen, U., Abbas, B. & Van Loosdrecht, M. C. M. Enrichment of DNRA bacteria in a continuous culture. *ISME J.* **9**, 2153–2161 (2015).
26. Reguera, G. & Kashefi, K. The electrifying physiology of Geobacter bacteria, 30 years on. *Adv. Microb. Physiol.* **74**, 1–96 (2019).
27. Zhao, Y. et al. Assembly mechanism and co-occurrence patterns of DNRA microbial communities and imprint of nitrate reduction in the Songhua River sediments of China's largest old industrial base. *J. Environ. Manag.* **322**, 116091 (2022).
28. Wan, Y. et al. Syntrophic growth of Geobacter sulfurreducens accelerates anaerobic denitrification. *Front. Microbiol.* **9**, 1572 (2018).
29. Zhou, L. et al. Identification of dissimilatory nitrate reduction to ammonium (DNRA) and denitrification in the dynamic cake layer of a full-scale anoixc dynamic membrane bioreactor for treating hotel laundry wastewater. *Chemosphere* **307**, 136078 (2022).
30. Zhu, Q. et al. Potassium channel blocker selectively enriched Geobacter from mixed-cultured electroactive biofilm: insights from microbial community, functional prediction and gene expressions. *Bioresour. Technol.* **364**, 128109 (2022).
31. Colatriano, D. et al. Genomic evidence for the degradation of terrestrial organic matter by pelagic Arctic Ocean Chloroflexi bacteria. *Commun. Biol.* **1**, 90 (2018).
32. Zhao, Y. et al. Genome-centered metagenomics analysis reveals the symbiotic organisms possessing ability to cross-feed with anammox bacteria in anammox consortia. *Environ. Sci. Technol.* **52**, 11285–11296 (2018).
33. Shi, J., Zhang, B., Cheng, Y. & Peng, K. Microbial vanadate reduction coupled to co-metabolic phenanthrene biodegradation in groundwater. *Water Res.* **186**, 116354 (2020).
34. Lovley, D. R. et al. Geobacter: the microbe electric's physiology, ecology, and practical applications. *Adv. Microb. Physiol*. **59**, 1–100 (2011).
35. Lovley, D. R. Happy together: microbial communities that hook up to swap electrons. *ISME J.* **11**, 327–336 (2017).
36. Guo, W. et al. Interspecies electron transfer between Geobacter and denitrifying bacteria for nitrogen removal in bioelectrochemical system. *Chem. Eng. J.* **455**, 139821 (2023).
37. Zhou, H. et al. Mechanisms of magnetic sensing and regulating extracellular electron transfer of electroactive bacteria under magnetic fields. *Sci. Total Environ.* **895**, 165104 (2023).
38. Yılmaz, H. et al. Nitrite is reduced by nitrite reductase NirB without small subunit NirD in Escherichia coli. *J. Biosci. Bioeng.* **134**, 393–398 (2022).
39. Wang, Z. et al. Widespread but overlooked DNRA process in a full-scale simultaneous partial nitrification, anammox, and denitrification plant. *ACS EST Water* **2**, 1360–1369 (2022).
40. Feng, Y. et al. Discrepant gene functional potential and cross-feedings of anammox bacteria Ca. Jettenia caeni and Ca. Brocadia sinica in response to acetate. *Water Res.* **165**, 114974 (2019).
41. Wang, C., Qiao, S., Bi, Z. & Zhou, J. Nitrate removal by anammox biomass with intracellular carbon source as electron donors via DNRA pathway. *Environ. Res.* **200**, 111390 (2021).
42. Li, J. et al. Successful application of anammox using the hybrid autotrophic-heterotrophic denitrification process for low-strength wastewater treatment. *Environ. Sci. Technol.* **56**, 13964–13974 (2022).
43. Fortin, S. G., Song, B. & Anderson, I. C. Microbially mediated nitrogen removal and retention in the York River Estuary. *FEMS Microbiol. Ecol.* **97**, fiab118 (2021).
44. Van Den Berg, E. M., Elisário, M. P., Kuenen, J. G., Kleerebezem, R. & Van Loosdrecht, M. C. M. Fermentative bacteria influence the competition between denitrifiers and DNRA bacteria. *Front. Microbiol.* **8**, 1–13 (2017).
45. Shuangyuan, L. et al. Dissimilatory nitrate reduction to ammonium (DNRA) and denitrification pathways are leveraged by cyclic AMP receptor protein (CRP) paralogues based on electron donor/acceptor limitation in shewanella loihica PV-4. *Appl. Environ. Microbiol.* **87**, e01964–20 (2021).
46. Zschiedrich, C. P., Keidel, V. & Szurmant, H. Molecular mechanisms of two-component signal transduction. *J. Mol. Biol.* **428**, 3752–3775 (2016).
47. Yan, H. J., Cui, Y. W. & Han, S. C. Promoting enrichment of sulfur-oxidizing autotrophic denitrifiers via static magnetic fields: performance and mechanism of magnetic biological effects. *Bioresour. Technol.* **347**, 126388 (2022).
48. Raina, J. B., Fernandez, V., Lambert, B., Stocker, R. & Seymour, J. R. The role of microbial motility and chemotaxis in symbiosis. *Nat. Rev. Microbiol.* **17**, 284–294 (2019).
49. Zhang, Y., Qiao, Y. & Fu, Z. Shifts of bacterial community and predictive functional profiling of denitrifying phosphorus removal – partial nitrification – anammox three-stage nitrogen and phosphorus removal before and after coupling for treating simulated wastewater with low C. *N. Chem. Eng. J.* **451**, 138601 (2023).
50. Sun, Y. et al. Chemotaxis mediates nitrogen acquisition of maize under long-term nitrogen input. *Soil Biol. Biochem.* **184**, 109118 (2023).
51. Van Steendam, C., Smets, I., Skerlos, S. & Raskin, L. Improving anaerobic digestion via direct interspecies electron transfer requires development of suitable characterization methods. *Curr. Opin. Biotechnol.* **57**, 183–190 (2019).
52. Liu, J. et al. Effect of temperature on fermentative VFAs production from waste sludge stimulated by riboflavin and the shifts of microbial community. *Water Sci. Technol.* **85**, 1191–1201 (2022).
53. Edel, M. et al. Extracellular riboflavin induces anaerobic biofilm formation in Shewanella oneidensis. *Biotechnol. Biofuels* **14**, 130 (2021).
54. Min, D. et al. Extracellular electron transfer via multiple electron shuttles in waterborne Aeromonas hydrophila for bioreduction of pollutants. *Biotechnol. Bioeng.* **118**, 4760–4770 (2021).
55. Huang, L., Liu, X., Ye, Y., Chen, M. & Zhou, S. Evidence for the coexistence of direct and riboflavin-mediated interspecies electron transfer in Geobacter co-culture. *Environ. Microbiol.* **22**, 243–254 (2020).
56. Huang, H., Chen, Y., Yang, S. & Zheng, X. CuO and ZnO nanoparticles drive the propagation of antibiotic resistance genes during sludge anaerobic digestion: possible role of stimulated signal transduction. *Environ. Sci. Nano* **6**, 528–539 (2019).
57. Zhu, Y., Dou, Q., Du, L. & Wang, Y. QseB/QseC: a two-component system globally regulating bacterial behaviors. *Trends Microbiol.* **31**, 749–762 (2023).
58. Mascher, T., Helmann, J. D. & Unden, G. Stimulus perception in bacterial signal-transducing histidine kinases. *Microbiol. Mol. Biol. Rev.* **70**, 910–938 (2006).
59. Yang, N. et al. Coupling mixotrophic denitrification and electroactive anodic nitrification by nitrate addition for promoting current generation and nitrogen removal. *Sci. Total Environ.* **856**, 159082 (2023).
60. Malvankar, N. S. & Lovley, D. R. Microbial nanowires for bioenergy applications. *Curr. Opin. Biotechnol.* **27**, 88–95 (2014).
61. Ha, P. T. et al. Syntrophic anaerobic photosynthesis via direct interspecies electron transfer. *Nat. Commun.* **8**, 13924 (2017).
62. Lojou, E., Cutruzzolà, F., Tegoni, M. & Bianco, P. Electrochemical study of the intermolecular electron transfer to Pseudomonas aeruginosa cytochrome cd1 nitrite reductase. *Electrochim. Acta* **48**, 1055–1064 (2003).
63. Pyun, S. I. Thermodynamic and electro-kinetic analyses of direct electron transfer (DET) and mediator-involved electron transfer (MET) with the help of a redox electron mediator. *J. Solid State Electrochem.* **24**, 2685–2693 (2020).
64. Matilla, M. A., Gavira, J. A. & Krell, T. Accessing nutrients as the primary benefit arising from chemotaxis. *Curr. Opin. Microbiol.* **75**, 102358 (2023).

65. Song, Z. et al. Facial fabricated biocompatible homogeneous biocarriers involving biochar to enhance denitrification performance in an anoxic moving bed biofilm reactor. *Bioresour. Technol.* **341**, 125866 (2021).
66. Wu, X. et al. Metagenomic insights into genetic factors driving bacterial niche differentiation between bulk and rhizosphere soils. *Sci. Total Environ.* **891**, 164221 (2023).
67. Sperandio, V., Torres, A. G. & Kaper, J. B. Quorum sensing Escherichia coli regulators B and C (QseBC): a novel two-component regulatory system involved in the regulation of flagella and motility by quorum sensing in E. coli. *Mol. Microbiol.* **43**, 809–821 (2002).
68. Jenal, U., Reinders, A. & Lori, C. Cyclic di-GMP: second messenger extraordinaire. *Nat. Rev. Microbiol.* **15**, 271–284 (2017).
69. Ren, T. et al. Diversified metabolism makes novel Thauera strain highly competitive in low carbon wastewater treatment. *Water Res.* **206**, 117742 (2021).
70. Ahmad, H. A. et al. A twilight for the complete nitrogen removal via synergistic partial-denitrification, anammox, and DNRA process. *npj Clean. Water* **4**, 31 (2021).
71. Decleyre, H., Heylen, K., Van Colen, C. & Willems, A. Dissimilatory nitrogen reduction in intertidal sediments of a temperate estuary: small scale heterogeneity and novel nitrate-to-ammonium reducers. *Front. Microbiol.* **6**, 1124 (2015).
72. Chen, R. et al. The pentatricopeptide repeat protein EMP601 functions in maize seed development by affecting RNA editing of mitochondrial transcript ccmC. *Crop J.* **11**, 1368–1379 (2023).
73. Wang, Z., Liu, X., Ni, S. Q., Zhuang, X. & Lee, T. Nano zero-valent iron improves anammox activity by promoting the activity of quorum sensing system. *Water Res.* **202**, 117491 (2021).
74. Gao, Y. et al. Understanding of the potential role of carbon dots in promoting interspecies electron transfer process in anaerobic co-digestion under magnetic field: focusing on methane and hydrogen production. *Chem. Eng. J.* **489**, 151381 (2024).
75. Pradhan, S. K., Mikola, A. & Vahala, R. Nitrogen and phosphorus harvesting from human urine using a stripping, absorption, and precipitation process. *Environ. Sci. Technol.* **51**, 5165–5171 (2017).
76. Cath, T. Y., Childress, A. E. & Elimelech, M. Forward osmosis: principles, applications, and recent developments. *J. Memb. Sci.* **281**, 70–87 (2006).
77. Wu, X. & Modin, O. Ammonium recovery from reject water combined with hydrogen production in a bioelectrochemical reactor. *Bioresour. Technol.* **146**, 530–536 (2013).
78. Kuntke, P. et al. Ammonium recovery and energy production from urine by a microbial fuel cell. *Water Res.* **46**, 2627–2636 (2012).
79. Zhou, L., Zhao, B. & Zhuang, W.-Q. Double-edged sword effects of dissimilatory nitrate reduction to ammonium (DNRA) bacteria on anammox bacteria performance in an MBR reactor. *Water Res.* **233**, 119754 (2023).
80. Zieliński, M. et al. Nitrification in activated sludge exposed to static magnetic field. *Water Air. Soil Pollut.* **228**, 126 (2017).
81. Dixon, M. A. & Abbas, T. R. Use of aerated magnetic biofilm reactor to treat wastewater. *Desalin. Water Treat.* **57**, 8061–8067 (2016).
82. Yavuz, C. T., Prakash, A., Mayo, J. T. & Colvin, V. L. Magnetic separations: from steel plants to biotechnology. *Chem. Eng. Sci.* **64**, 2510–2521 (2009).
83. Ahmad, H. A. et al. Multi-omics analysis revealed the selective enrichment of partial denitrifying bacteria for the stable coupling of partial-denitrification and anammox process under the influence of low strength magnetic field. *Water Res.* **245**, 120619 (2023).
84. Liu, S., Yang, F., Meng, F., Chen, H. & Gong, Z. Enhanced anammox consortium activity for nitrogen removal: impacts of static magnetic field. *J. Biotechnol.* **138**, 96–102 (2008).
85. Braker, G., Zhou, J., Wu, L., Devol, A. H. & Tiedje, J. M. Nitrite reductase genes (nirK and nirS) as functional markers to investigate diversity of denitrifying bacteria in pacific northwest marine sediment communities. *Appl. Environ. Microbiol.* **66**, 2096–2104 (2000).
86. Welsh, A., Chee-Sanford, J. C., Connor, L. M., Löffler, F. E. & Sanford, R. A. Refined NrfA phylogeny improves PCR-based nrfA gene detection. *Appl. Environ. Microbiol.* **80**, 2110–2119 (2014).
87. Minoru, K., Miho, F., Mao, T., Yoko, S. & Kanae, M. KEGG: new perspectives on genomes, pathways, diseases and drugs. *Nucleic Acids Res.* **45**, D353–D361 (2017).

Acknowledgements

The authors gratefully acknowledge the support from the National Natural Science Foundation of China (22076100, 52250410337, 52311540153), Taishan Scholar Youth Expert Program of Shandong Province (tsqn201909005), Instrument Improvement Funds of Shandong University Public Technology Platform (ts20220106) and Jinan Science and Technology Research Project (202221004, 202221005).

Author contributions

S. N. contributed to supervision, funding acquisition, writing-reviewing & editing. Y. X. performed material preparation, data collection, and analysis. Z. W. contributed to writing-reviewing and editing.

Competing interests

The authors declare no competing interests.

Additional information

Supplementary information The online version contains supplementary material available at https://doi.org/10.1038/s41545-024-00352-3.

Correspondence and requests for materials should be addressed to Shou-Qing Ni.